BIOCHEMISTRY
including biophysical chemistry & molecular biology

Article

pubs.acs.org/biochemistry

Analysis of the Intrinsically Disordered N-Terminus of the DNA Junction-Resolving Enzyme T7 Endonuclease I: Identification of Structure Formed upon DNA Binding

Alasdair D. J. Freeman,[†] Michael Stevens,[†] Anne-Cecile Declais,[†] Adam Leahy,[†] Katherine Mackay,[†] Hassane El Mkami,[‡] David M. J. Lilley,[†] and David G. Norman*[,†]

[†]Nucleic Acid Structure Research Group, College of Life Sciences, University of Dundee, Dow Street, Dundee DD1 5EH, U.K.
[‡]School of Physics and Astronomy, University of St Andrews, St Andrews FE2 4KM, U.K.

Supporting Information

ABSTRACT: The four-way (Holliday) DNA junction of homologous recombination is processed by the symmetrical cleavage of two strands by a nuclease. These junction-resolving enzymes bind to four-way junctions in dimeric form, distorting the structure of the junction in the process. Crystal structures of T7 endonuclease I have been determined as free protein, and the complex with a DNA junction. In neither crystal structure was the N-terminal 16-amino acid peptide visible, yet deletion of this peptide has a marked effect on the resolution process. Here we have investigated the N-terminal peptide by inclusion of spin-label probes at unique sites within this region, studied by electron paramagnetic resonance. Continuous wave experiments show that these labels are mobile in the free protein but become constrained on binding a DNA junction, with the main interaction occurring for residues 7−10 and 12. Distance measurements between equivalent positions within the two peptides of a dimer using PELDOR showed that the intermonomeric distances for residues 2−12 are long and broadly distributed in the free protein but are significantly shortened and become more defined on binding to DNA. These results suggest that the N-terminal peptides become more organized on binding to the DNA junction and nestle into the minor grooves at the branchpoint, consistent with the biochemical data indicating an important role in the resolution process. This study demonstrates the presence of structure within a protein region that cannot be viewed by crystallography.

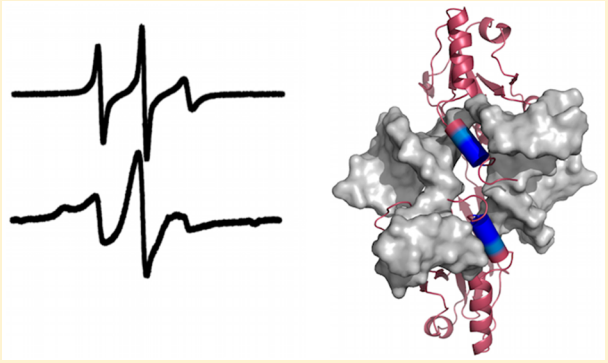

The DNA four-way (Holliday) junction is an essential intermediary structure in homologous recombination.[1−3] This process is important in repair of double-strand breaks in DNA, and in meiosis in eukaryotes. Resolution into unconnected duplex species requires recognition and cleavage of the four-way DNA junction in a structure-selective and concerted manner.[4] Phage T7 endonuclease I is a strongly associated homodimer comprising 149 amino acids per monomer.[5−7] The protein binds DNA four-way junctions with a dissociation constant of ∼1 nM.[8] Although the enzyme is selective for the structure of the junction (with a very weak sequence preference), the DNA structure is significantly altered on binding. Endonuclease I introduces two diametrically symmetrical cleavages to generate a productive resolution. The cleavages are sequential, rather than simultaneous, and yet concerted.[9] As a class, the junction-resolving enzymes generally ensure bilateral cleavages occur within the lifetime of the complex by acceleration of second-strand cleavage,[10−12] probably as a consequence of the structural distortion imposed.

Several crystallographic studies have defined the basic structures of endonuclease I in isolation[13,14] and in complex with a small four-way DNA junction.[15] There is limited flexibility in the endonuclease I dimer, and only a small conformational change takes place on binding to a four-way DNA junction.[15,16] Residues from both polypeptides contribute to each active site of endonuclease I (Asp55, Glu55, and Lys67 from monomer A and Glu20 from monomer B), and two metal ions are present in each.[17] The DNA−protein complex is held together by a combination of interactions with basic residues of the protein and also direct contacts between the DNA backbone and the active site metal ions.[17] There are two 30 Å long mutually perpendicular channels within the protein dimer, to which both polypeptides contribute. These are each occupied by coaxially aligned pairs of helical arms of the junction, thus explaining the selectivity of the enzyme for a junction that can adopt that disposition of helices, as observed in solution studies.[18]

Biochemical studies have defined an important role for the 16 N-terminal amino acids of endonuclease I.[19] Deletion of the N-termini led to increased affinity of binding, but a slower rate

Received: March 16, 2016
Revised: June 14, 2016
Published: July 7, 2016

DOI: 10.1021/acs.biochem.6b00242
Biochemistry 2016, 55, 4166−4172

of cleavage. Spectroscopic study indicated that these peptides are involved in an opening of the DNA structure at the center of the junction, and that their deletion resulted in substantially lowered bilateral cleavage. These results indicate a key role for the N-termini in the function of the enzyme, stabilizing the transition state and destabilizing the ground state. However, the N-terminal peptides could not be located within the electron density maps of either free or DNA-bound endonuclease I.[13,15] This presents a conundrum because the N-termini clearly play an important functional role but are not localized within the structure in the ground state.

In an effort to resolve this apparent contradiction, we have used site-directed spin labeling (SDSL),[20] continuous wave (CW) electron paramagnetic resonance (EPR),[21] and pulsed electron−electron double resonance (PELDOR) EPR[22,23] experiments to probe the environment and structural relationships of these amino acids more closely. We have constructed full-length endonuclease I single-point variants containing cysteine residues at positions 2, 6−10, 12, 14, 16, and 29 (Figure 1). The choice of positions to label was made to provide alternate residue coverage over the N-terminal region with emphasis on the region between residues 6 and 16. Initially, the rational was to avoid mutating large hydrophobic residues such as F15. Some extra sites were added later to provide greater coverage. Covalent attachment of the spin-label (1-oxyl-2,2,5,5-tetramethylpyrroline-3-methyl) methanethiosulfonate (MTSSL) at the sulfhydryl groups of these unique cysteine residues has allowed us to introduce the spin-label (R1) and to analyze the structure and dynamics of the N-terminal region using EPR.

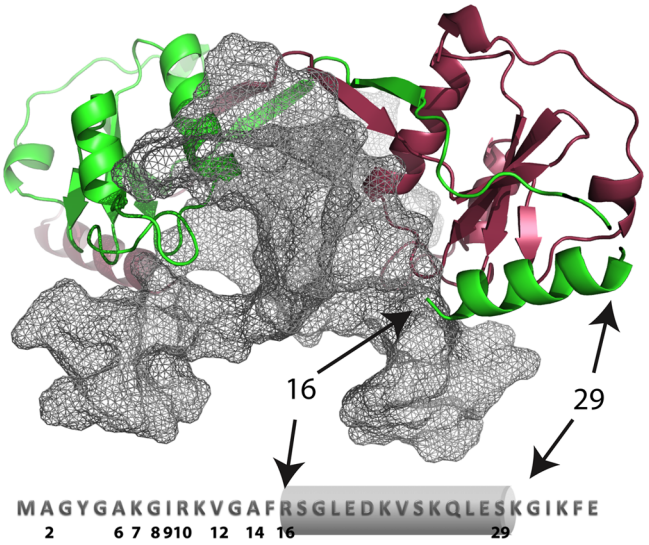

Figure 1. Known structure of endonuclease I (separate monomers shown as red and green cartoons). The DNA junction is shown as a gray surface. The structurally undetermined N-terminal sequence (residues 1−16) and the first helix (gray shading) with numbers indicating the positions studied by spin labeling. Residues 16 and 29 are indicated, for guidance, with arrows.

The shape of the CW nitroxide spectra recorded for the uniquely labeled sites depends on a number of factors, one of which is the dynamics of the label. Under suitable conditions, analysis of the shape of the spectrum can reveal the dynamic state of the spin-label, up to and including states in which the nitroxide is effectively immobile as a result of direct interaction with structured components of either the DNA junction or the protein. PELDOR can be used to measure long-range distances between unpaired electrons, in the range of 20−120 Å[24] or longer. Because endonuclease I forms a symmetrical dimer, single spin-labels attached to unique positions on the monomer produce a symmetrical pair of label sites within the dimer. The data obtained from both CW and PELDOR experiments indicate that the N-terminus is mobile in the free protein but becomes structured upon binding to the DNA junction.

EXPERIMENTAL PROCEDURES

Preparation of Endonuclease I. Site-directed mutagenesis of the N-terminal residues into cysteines was performed by polymerase chain reaction on the gene encoding endonuclease I, cloned in expression vector pET19-endoI using the QuickChange procedure (Stratagene). In each case, pairs of complementary mutagenic oligonucleotides were annealed to the double-stranded plasmid and then fully resynthesized with the *Pfu* polymerase. The parental DNA was removed by digestion with the methylation-sensitive restriction enzyme *Dpn*I, and the newly synthesized mutant plasmid was transformed into *Escherichia coli*. Each plasmid DNA was purified and sequenced before expression.

Endonuclease I was expressed in *E. coli* BL21(DE3)pLysS at 37 °C and grown to an absorbance A_{600} of 0.6, using plasmid pET19endo I prepared as described previously.[14] After induction with 0.1 mM isopropyl β-D-1-thiogalactopyranoside and further incubation at 30 °C for 4 h, the cells were harvested by centrifugation. Cells were resuspended in 5 volumes of PS buffer [50 mM sodium phosphate (pH 8) and 1 M NaCl] supplemented with the complete protease inhibitor cocktail (Roche) and lysed by sonication. The lysates were cleared by centrifugation at 45000*g* for 30 min and applied to a nickel-loaded HisTrap HP column (GE Healthcare). The N-terminal oligo-histidine-tagged protein was eluted using a 10 to 500 mM imidazole gradient in PS buffer. The histidine tag was removed from endonuclease I by digestion with TEV protease. The pure protein was extensively dialyzed against 50 mM Tris-HCl (pH 8), 100 mM NaCl, and 1 mM dithiothreitol. Protein concentrations were measured optically, using an absorption coefficient of 49500 M^{-1} cm^{-1} at 280 nm for a dimer of endonuclease I.

Before labeling, the cysteine residues were fully reduced by adding 20 mM dithiothreitol to the protein sample, and the excess reducing agent was removed by anion exchange chromatography on Sephadex SP (GE Healthcare). The proteins were reacted with a 10-fold excess of MTSSL at a protein concentration of 20−100 μM dimer for 1 h at 4 °C. Unreacted MTSSL was removed by dialysis against water, and protein samples were lyophilized prior to use. Derivatization of endonuclease I by MTSSL was verified by measurement of the increase in molecular mass using mass spectroscopy.

DNA Synthesis. Oligodeoxynucleotides were synthesized by phosphoramidite chemistry on a 394 DNA/RNA synthesizer (Applied Biosystems).[25,26] Fully deprotected oligonucleotides were purified by gel electrophoresis in polyacrylamide gels [10−20% (w/v)] in 90 mM Tris-borate (pH 8.5) and 2 mM EDTA (TBE buffer) containing 8 M urea and recovered by electroelution and ethanol precipitation. Four-way junctions were assembled by mixing stoichiometric quantities of four strands and annealed by incubation in 20 mM Tris-HCl (pH 8) and 50 mM NaCl for 5 min at 85 °C, followed by slow cooling. DNA junctions were purified by gel electrophoresis in

DOI: 10.1021/acs.biochem.6b00242
Biochemistry 2016, 55, 4166−4172

polyacrylamide under nondenaturing conditions and eluted from excised gel fragments by diffusion into buffer. The DNA was ethanol precipitated before being resuspended in D_2O.

Preparation of EPR Samples. For PELDOR experiments, spin-labeled, lyophilized protein was resuspended in 50 μL of D_2O containing 20 mM HEPES (pH 7.5) buffer, 100 mM NaCl, and 20 mM $CaCl_2$ (note the use of Ca^{2+} ions rather than Mg^{2+} ions leads to proteins that are structurally stable but catalytically inactive) and then diluted with an equal volume of d_8-glycerol (50 μL) to produce a final volume of 100 μL. Samples typically had concentrations of 100 μM. When required, DNA junction was added as a concentrated solution in D_2O directly to the protein, prior to the addition of glycerol. Samples for CW spectroscopy were prepared in the same buffer and at the same concentration as PELDOR samples but without deuteration and with the addition of Ficol 70 to a concentration of 25% to increase sample viscosity.[27]

PELDOR Experiments. Experiments were performed using a Bruker ELEXSYS E580 spectrometer operating at X-band with a dielectric ring resonator and a Bruker 400U second microwave source unit. All measurements were taken at 50 K with an overcoupled resonator giving a Q factor of <100. The video bandwidth was set to 20 MHz. The four-pulse, dead-time free PELDOR sequence was used, with the pump pulse frequency positioned at the center of the nitroxide spectrum. The frequency of the observer pulses was incremented, by 80 MHz relative to the pump position. The observer sequence used a 32 ns π-pulse; the pump $\pi/2$-pulse was typically 16 ns. The experiment repetition time was 4 μs, and the number of shots at each time point was 50. The number of time points and the number of scans used were varied for each sample, but sufficient data were collected to obtain an acceptable signal-to-noise ratio.

PELDOR Data Analysis. Data were analyzed using the DeerAnalysis 2006 software package.[28] In brief, the dipolar coupling evolution data were corrected for background echo decay using a homogeneous three-dimensional spin distribution. The starting time for the background fit was optimized to give the best-fit Pake pattern in the Fourier-transformed data and the lowest root-mean-square deviation background fit. Tikhonov regularization was used to derive distance distributions $P(r)$.

CW EPR Experiments. Continuous wave (CW) EPR was performed at X-band with a constant frequency of 9.876 GHz. Spectra were recorded on a Bruker EMX spectrometer working at X-band using a super-high-sensitivity probe head (Bruker ER4122SHQE resonator). CW EPR was performed in a critically coupled resonator with a typical Q factor of 7000. Data were collected over a magnetic field range of 100 G centered at 3519.1 G using a constant microwave frequency of 9.876 GHz. Background noise was averaged out over 10 sweeps at a power of 10 mW, and spectra were normalized so their central peaks were all equivalent.

RESULTS AND DISCUSSION

Comparative Spin-Label Dynamics Revealed by CW EPR. The CW EPR traces of the R1 spin-label attached at various positions on the N-terminus of endonuclease I are shown in Figure 2. Experiments were conducted on free protein or that bound to a DNA four-way junction (S2). Initial examination of the CW spectra revealed significant differences between DNA-bound and unbound states, at most sites in the N-terminus of endonuclease I.

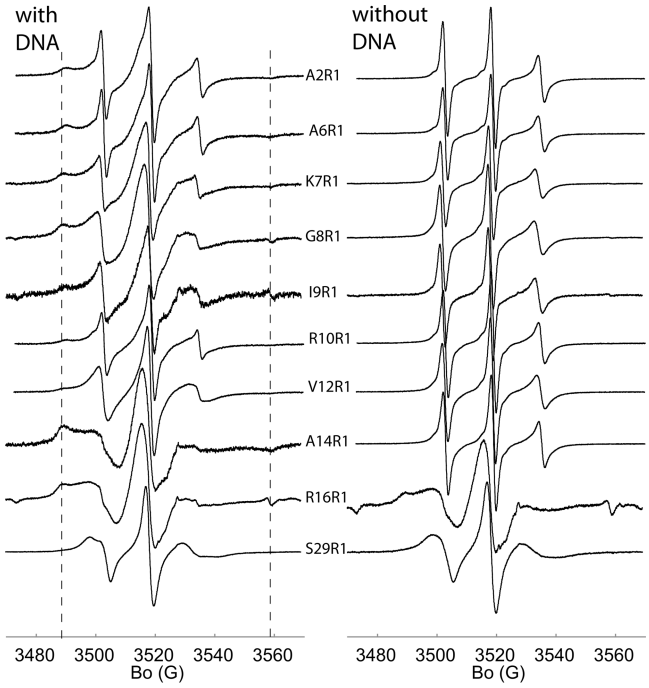

Figure 2. CW spectra recorded on endonuclease I, with spin-labels attached at positions 2, 6−10, 12, 14, 16, and 29: (left column) bound to DNA junction and (right column) free protein. Positions 3489G and 3559G are indicated with dashed lines.

The most obvious differences between free protein and that which is DNA-bound include a considerable broadening of the lines on going from the unbound to the DNA-bound state and the appearance of a new peak at low field (3489G) and a smaller high-field peak (3559G). The broadening effect is indicative of a decrease in the level of dynamic motion of the spin-label ($\tau \sim 5$ ns) upon binding to the DNA junction. The appearance of the extreme low-field and high-field peaks indicates that the environment of the spin-label results in at least some of the label population becoming relatively immobilized, such that its dynamic properties are those of the overall tumbling of the complex ($\tau > 50$ ns). Attempts to fit the CW spectra using EasySpin[29] were unsuccessful, and a reasonable interpretation could be that the nitroxide spectra are strongly multicomponent.

The analysis of mobility from CW spectra can be complicated by the presence of multiple conformational forms. The data shown in Figure 3 provide some indication of the proportion of the immobile form of the spin-label in the N-terminal region, when the endonuclease I is bound to a DNA junction, probably indicating the proximity of the spin-labels to the DNA. The absence of the corresponding peaks in the spectra of unbound endonuclease I also illustrates the disordered nature of the N-terminal region in the absence of DNA. Because the CW spectra are reporting on the dynamics of spin-labels that are undoubtedly structurally heterogeneous, the interpretation of an individual spectral characteristic can be misleading; however, qualitative comparison between the DNA-bound and the free forms strongly indicates that the N-terminal region of the protein is highly mobile in the absence of DNA binding and becomes less mobile when bound to DNA, with a portion being very immobile. As indicated by the PELDOR measurements, discussed in the next section, the spin-labels at the extreme N-terminus are very close to each

DOI: 10.1021/acs.biochem.6b00242
Biochemistry 2016, 55, 4166−4172

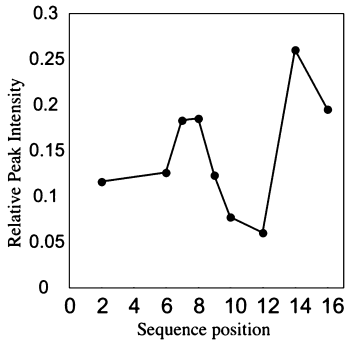

Figure 3. Graph showing the relative intensity of the low-field peak (corresponding to an immobilized spin-label) in normalized spectra, as a function of sequence position in the N-terminal peptide in endonuclease I bound to the DNA junction.

other within the protein dimer. The CW spectra of the DNA-bound complex are all significantly broadened relative to those of the non-DNA-bound form, indicating a relatively slow motion, within at least some of the conformations. It is possible that the extreme N-terminal spin-labels could be close enough to be broadened by dipolar coupling and so could be more mobile than the CW spectra might imply. The presence of a low-field peak in these spectra does, however, suggest that some proportion of the N-terminus is essentially immobile, making it likely that extreme N-terminal labels are indeed exist in either a slow or very slow motional regime.

Distance Measurement by PELDOR. Using the same spin-labeled species that were previously analyzed by CW EPR, we have measured the distance between the two labels within the dimeric complex of endonuclease I using the PELDOR experiment, which exploits the distance dependence of dipolar coupling between spin-labels.[30−32] When spin-labels are held in structurally homogeneous positions and the background signal is removed, the spin echo of the PELDOR pulse sequence exhibits oscillation revealing the dipolar coupling frequency, which can yield the distance distribution between labels. If underlying structures are less well-defined, with some level of structural heterogeneity, the dipolar oscillations will be subject to a degree of interference and cancellation, leading to a damping of the echo oscillation, thus rendering the determination of accurate distance (or distance distribution) problematic. Initial decay of the PELDOR signal reveals an average spin−spin distance relationship even in the absence of a persistent measurable echo oscillation. Labels at positions 12, 14, and 16 gave PELDOR signals with observable oscillations. PELDOR data for all other label positions were largely free of oscillation, after the initial decay. All baseline-corrected data were transformed to distance distributions using Tikhonov regularization within DeerAnalysis (Figure 4). Distance distributions from data that are essentially free of oscillations should be interpreted with care; however, comparison across all label positions is instructive as is the average distance measurement that can be made from the initial slope in the baseline-corrected data (Table 1 and Figure 5).

The PELDOR-derived distances clearly exhibit significant differences between DNA-bound and unbound forms of the protein. In the absence of bound DNA, data from spin-labels, up to and including position 12, show very long distances with extremely broad distributions, consistent with a largely disordered structure.[33] Binding to the DNA junction causes the spin−spin distances to be shortened significantly, with the

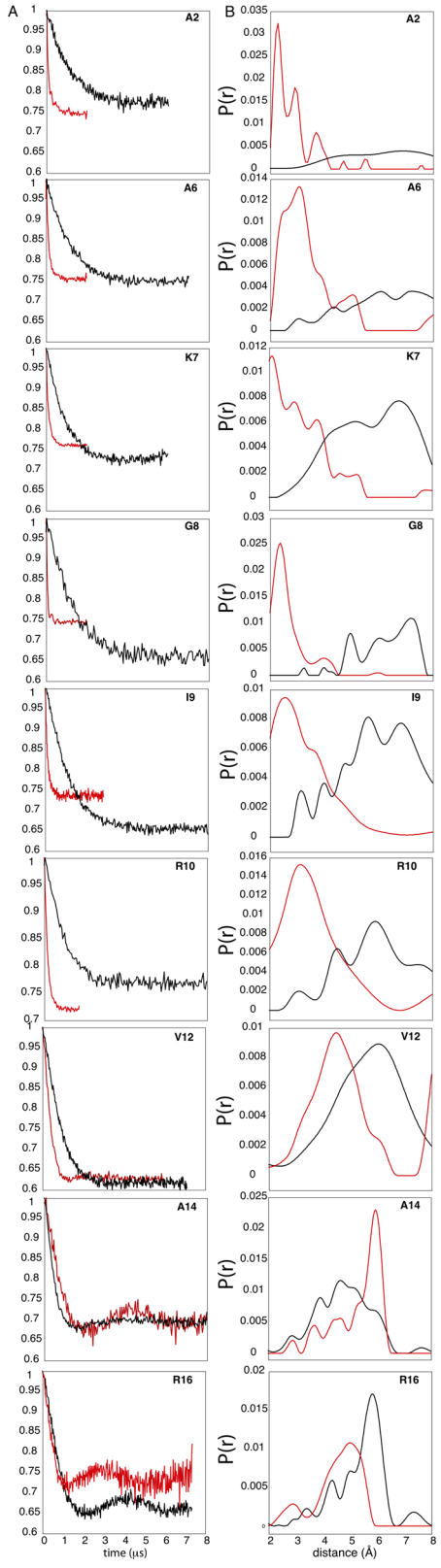

Figure 4. PELDOR data and derived distance distributions for spin-labeled endonuclease I in the presence (red) and absence (black) of a bound DNA junction. (A) Background-corrected data and (B) distance distributions calculated using Tikhonov regularization. Axes for background-corrected data are normalized intensity, and for the distributions, axes are $P(r)$, the distance probability.

DOI: 10.1021/acs.biochem.6b00242
Biochemistry 2016, 55, 4166−4172

Table 1. Distances Derived from the PELDOR Data[a]

amino acid position	distance without DNA (nm)	distance with DNA (nm)
2	5.6	2.7
6	5.8	2.8
7	5.6	2.6
8	6.1	2.3
9	5.9	2.8
10	5.6	3.2
12	5.6	4.5
14	4.5	5.9
16	5.8	4.9

[a]The values shown are the average values derived from the initial slopes of the background-corrected PELDOR data.

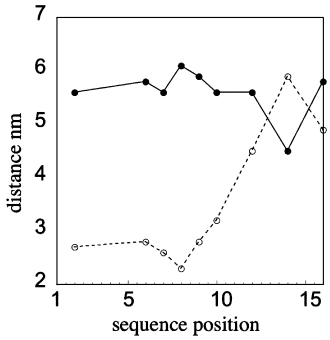

Figure 5. Plot of the estimated spin−spin distance as a function of the position of the spin-labels in the protein sequence. Distances calculated in the absence of bound DNA (—, ●) and in the presence of bound DNA (---, ○).

distance between labels being reduced from position 14 to position 8 and then leveling off at distances of <25 Å. The distance distributions for the DNA-bound forms are still broad, although from position 8 onward the distributions become sharper with positions 14 and 16 being much better defined.

In the X-ray diffraction-determined structure [Protein Data Bank (PDB) entry 2PFJ] of the DNA-bound protein, the N-terminal helices from residue 29 to 17 are directed toward each other underneath the bound DNA junction. Residues from position 17 to 1 did not show sufficient electron density to define structure. The CW and PELDOR data both indicate that, in the absence of bound DNA, the N-terminal residues before residue 16 are highly mobile and structurally disordered. The data from the DNA-bound complex indicate a much less mobile condition for the 12 N-terminal residues. The presence of peaks in the CW spectra (of the DNA-bound form) at around 3489G indicates a degree of immobility probably due to direct contact by the spin-labels in the N-terminal region with the DNA. The 3489G peak is present in all CW spectra derived from the protein−DNA complex and absent in all CW spectra taken of the protein alone (except residue 16) (Figure 2). Comparison of the CW spectra, between DNA-bound and nonbound constructs, implies a general decrease in the mobility of the DNA-bound forms as judged by the broadening of the lines; however, the inferred decrease in mobility is uneven through the N-terminal sequence with the mobility of residues at positions 2 and 6 approaching that of the non-DNA-bound form while still exhibiting a peak at 3489G, indicating that some portion of the spin-label is relatively immobile.

The distances taken from the PELDOR experiments indicate a generally decreasing distance between the symmetry-related spin-labels as one moves from residue 14 to 8. From residue 8 to 2, the distance between spin-labels changes very little, around a value of ∼2.5 Å.

Structural conclusions from the described EPR data are bound to be somewhat speculative; however, we can suggest that given the presence of immobile spin-label species within the N-terminal sequence (in the DNA-bound complex) and the range of distance distributions observed between symmetrically located spin-labels, the N-terminal region under these conditions must be taking on a more compact and less dynamic structure than when in the non-DNA-bound state. The restraints imposed by the structure of the bound DNA, the CW spectra, and the distance measurements made from PELDOR suggest that the N-terminal peptides extend from the last crystallographically determined residue, R16, into the widened minor grooves at the center of the DNA junction (Figure 6). Because the distance measurements show a crossing

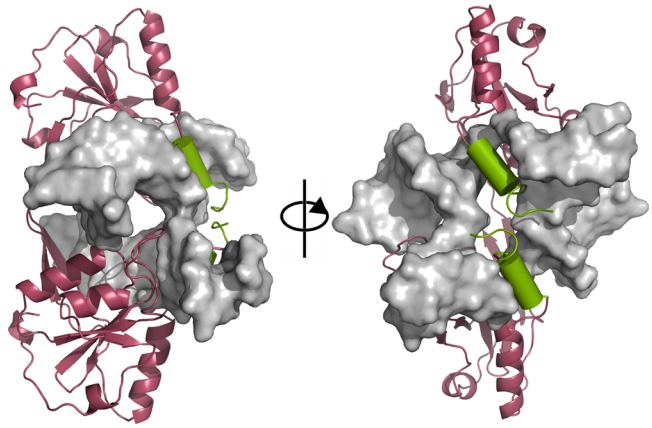

Figure 6. Two views of the endonuclease I dimer (magenta cartoon representation with crystallographically determined helices and strands) bound to a four-way DNA junction (gray surface representation) (PDB entry 2PFJ). A putative position for the 16 N-terminal residues is shown crossing the underside of the junction (green cylinder).

of the dimerically related N-terminal regions (Figure 5), with the distances from PELDOR evening out at approximately 2.6−2.8 Å for residues below position 8, and because the pattern of dynamic changes was observed in the CW spectra, it can be suggested that the peptides must adopt a somewhat compact structure pointing in toward the protein's dyad axis. The dimensions of the DNA surface into which this N-terminal region is pointing could accommodate a helical structure, although the data do not provide the resolution to predict this with great certainty.

The total deletion of the N-terminus of endonuclease I has previously been shown to have a marked effect on several structural and functional features.[19] Binding between the protein and the DNA becomes stronger, and cleavage becomes slower. A large change in activation energy is measured, and although the overall shape of the complex remains unaffected, it was noticed that there was an almost total suppression of the 2-aminopurine fluorescence enhancement normally observed, resulting from the opening of the center of the DNA junction. The most striking change observed is perhaps the switch from bilateral to unilateral DNA cleavage in supercoiled substrate. This may be explained by the slower cleavage rate or may be due to more subtle changes in the reaction trajectory.

DOI: 10.1021/acs.biochem.6b00242
Biochemistry 2016, 55, 4166−4172

All crystallographically studied junction-resolving enzymes present a large, 2-fold symmetrical, basic surface, which is expected to bind the four-way junction. Apart from endonuclease I, these surfaces all present some protruding structural elements at the dyad axis of the dimer that are expected to be inserted into the center of the junction upon binding.[4] This has been confirmed in all cocrystal structures to date, with α-helices and adjacent loops playing this role in T4 endonuclease VII,[34] RuvC,[35] and GEN1.[36] These domains are often disordered and expected to be dynamic in the free protein, but they may become more ordered upon substrate binding. In this context, our results suggest that the N-terminus of endonuclease I plays a similar role by inserting into the minor grooves at the branchpoint. However, endonuclease I is unique in that it wraps around the center of the junction and the N-termini bind the other face of the substrate rather than forming a protrusion in the main DNA-binding surface.

In conclusion, we have observed the disordered nature of the N-terminal region of endonuclease I in the absence of a bound DNA junction and the formation of structure within those residues upon binding to a DNA junction. The structure formed does not appear to be ordered enough to give interpretable electron density from X-ray diffraction but is ordered enough to show significant changes in the CW spectra of site specifically labeled positions in the N-terminal region and also to give more defined and shorter distance distributions in PELDOR experiments. On the basis of the constraints imposed by the distance measurements and the symmetrical nature of the structure, we propose that the N-terminal region must form a structure that is inserted into the minor groove at the junction branchpoint and play a key role in its opening.

■ ASSOCIATED CONTENT

Supporting Information

The Supporting Information is available free of charge on the ACS Publications website at DOI: 10.1021/acs.biochem.6b00242.

DNA oligomers used to construct the four-way junction and activity of mutant and spin-labeled mutant endonuclease I (PDF)

■ AUTHOR INFORMATION

Corresponding Author

*Nucleic Acid Structure Research Group, College of Life Sciences, University of Dundee, Dow Street, Dundee DD1 5EH, U.K. E-mail: d.g.norman@dundee.ac.uk. Phone: +44(0) 1382 384798.

Author Contributions

A.D.J.F. and M.S. contributed equally to this work.

Funding

This work was supported by grants from The Engineering and Physical Sciences Research Council (EPSRC), Basic Technology EP/F039034/1, The Wellcome Trust, 099149/Z/12/Z, and Cancer Research UK (CRUK), C28/A18604.

Notes

The authors declare no competing financial interest.

■ ACKNOWLEDGMENTS

The authors acknowledge preliminary work performed by Mr. Max Byrne and assistance with CW provided by Dr. David Keeble.

■ ABBREVIATIONS

EPR, electron paramagnetic resonance; PELDOR, pulsed electron−electron double resonance; CW, continuous wave.

■ REFERENCES

(1) Schwacha, A., and Kleckner, N. (1995) Identification of Double Holliday Junctions as Intermediates in Meiotic Recombination. *Cell 83*, 783−791.

(2) Holliday, R. (1964) Mechanism for Gene Conversion in Fungi. *Genet. Res. 5*, 282.

(3) Potter, H., and Dressler, D. (1976) Mechanism of Genetic-Recombination - Electron-Microscopic Observation of Recombination Intermediates. *Proc. Natl. Acad. Sci. U. S. A. 73*, 3000−3004.

(4) Declais, A. C., and Lilley, D. M. J. (2008) New insight into the recognition of branched DNA structure by junction-resolving enzymes. *Curr. Opin. Struct. Biol. 18*, 86−95.

(5) Center, M. S., and Richards, Cc. (1970) Endonuclease Induced after Infection of Escherichia-Coli with Bacteriophage-T7 0.1. Purification and Properties of Enzyme. *J. Biol. Chem. 245*, 6285.

(6) Center, M. S., and Richards, Cc. (1970) Endonuclease Induced after Infection of Escherichia-Coli with Bacteriophage-T7 0.2. Specificity of Enzyme toward Single- and Double-Stranded Deoxy-ribo-Nucleic Acid. *J. Biol. Chem. 245*, 6292.

(7) Center, M. S., Studier, F. W., and Richardson, C. C. (1970) Structural Gene for a T7-Endonuclease Essential for Phage DNA Synthesis. *Proc. Natl. Acad. Sci. U. S. A. 65*, 242.

(8) Declais, A. C., Liu, J., Freeman, A. D. J., and Lilley, D. M. J. (2006) Structural recognition between a four-way DNA junction and a resolving enzyme. *J. Mol. Biol. 359*, 1261−1276.

(9) Parkinson, M. J., and Lilley, D. M. J. (1997) The junction-resolving enzyme T7 endonuclease 0.1. Quaternary structure and interaction with DNA. *J. Mol. Biol. 270*, 169−178.

(10) Fogg, J. M., Schofield, M. J., Declais, A. C., and Lilley, D. M. J. (2000) Yeast resolving enzyme CCE1 makes sequential cleavages in DNA junctions within the lifetime of the complex. *Biochemistry 39*, 4082−4089.

(11) Fogg, J. M., and Lilley, D. M. J. (2000) Ensuring productive resolution by the junction-resolving enzyme RuvC: Large enhancement of the second-strand cleavage rate. *Biochemistry 39*, 16125−16134.

(12) Freeman, A. D. J., Liu, Y., Declais, A. C., Gartner, A., and Lilley, D. M. J. (2014) GEN1 from a Thermophilic Fungus Is Functionally Closely Similar to Non-Eukaryotic Junction-Resolving Enzymes. *J. Mol. Biol. 426*, 3946−3959.

(13) Hadden, J. M., Convery, M. A., Declais, A. C., Lilley, D. M. J., and Phillips, S. E. V. (2001) Crystal structure of the Holliday junction resolving enzyme T7 endonuclease I. *Nat. Struct. Biol. 8*, 62−67.

(14) Hadden, J. M., Declais, A. C., Phillips, S. E., and Lilley, D. M. (2002) Metal ions bound at the active site of the junction-resolving enzyme T7 endonuclease I. *EMBO J. 21*, 3505−3515.

(15) Hadden, J. M., Declais, A. C., Carr, S. B., Lilley, D. M., and Phillips, S. E. (2007) The structural basis of Holliday junction resolution by T7 endonuclease I. *Nature 449*, 621−624.

(16) Freeman, A. D. J., Ward, R., El Mkami, H., Lilley, D. M. J., and Norman, D. G. (2011) Analysis of Conformational Changes in the DNA Junction-Resolving Enzyme T7 Endonuclease I on Binding a Four-Way Junction Using EPR. *Biochemistry 50*, 9963−9972.

(17) Freeman, A. D., Declais, A. C., and Lilley, D. M. (2003) Metal ion binding in the active site of the junction-resolving enzyme T7 endonuclease I in the presence and in the absence of DNA. *J. Mol. Biol. 333*, 59−73.

(18) Declais, A. C., Fogg, J. M., Freeman, A. D. J., Coste, F., Hadden, J. M., Phillips, S. E. V., and Lilley, D. M. J. (2003) The complex between a four-way DNA junction and T7 endonuclease I. *EMBO J. 22*, 1398−1409.

(19) Freeman, A. D. J., Declais, A. C., and Lilley, D. M. J. (2013) The Importance of the N-Terminus of T7 Endonuclease I in the Interaction with DNA Junctions. *J. Mol. Biol. 425*, 395−410.

DOI: 10.1021/acs.biochem.6b00242
Biochemistry 2016, 55, 4166−4172

(20) Todd, A. P., Cong, J., Levinthal, F., Levinthal, C., and Hubell, W. L. (1989) Site-directed mutagenesis of colicin E1 provides specific attachment sites for spin labels whose spectra are sensitive to local conformation. *Proteins: Struct., Funct., Genet. 6*, 294−305.
(21) Hubbell, W. L., Mchaourab, H. S., Altenbach, C., and Lietzow, M. A. (1996) Watching proteins move using site-directed spin labeling. *Structure 4*, 779−783.
(22) Milov, A. D., Salikohov, K. M., and Shirov, M. D. (1981) Application of Endor in Electron-Spin Echo for Paramagnetic Center Space Distribution in Solids. *Fizika Tverdogo Tela 23*, 975−982.
(23) Pannier, M., Veit, S., Godt, A., Jeschke, G., and Spiess, H. W. (2000) Dead-time free measurement of dipole-dipole interactions between electron spins. *J. Magn. Reson. 142*, 331−340.
(24) El Mkami, H., and Norman, D. G. (2015) Chapter Five-EPR Distance Measurements in Deuterated Proteins. *Methods Enzymol. 564*, 125−152.
(25) Beaucage, S. L., and Caruthers, M. H. (1981) Deoxynucleoside Phosphoramidites - a New Class of Key Intermediates for Deoxypolynucleotide Synthesis. *Tetrahedron Lett. 22*, 1859−1862.
(26) Sinha, N. D., Biernat, J., Mcmanus, J., and Koster, H. (1984) Polymer Support Oligonucleotide Synthesis 0.18. Use of Beta-Cyanoethyl-N,N-Dialkylamino-/N-Morpholino Phosphoramidite of Deoxynucleosides for the Synthesis of DNA Fragments Simplifying Deprotection and Isolation of the Final Product. *Nucleic Acids Res. 12*, 4539−4557.
(27) Lopez, C. J., Fleissner, M. R., Guo, Z. F., Kusnetzow, A. K., and Hubbell, W. L. (2009) Osmolyte perturbation reveals conformational equilibria in spin-labeled proteins. *Protein Sci. 18*, 1637−1652.
(28) Jeschke, G., Chechik, V., Ionita, P., Godt, A., Zimmermann, H., Banham, J., Timmel, C. R., Hilger, D., and Jung, H. (2006) DeerAnalysis2006 - a comprehensive software package for analyzing pulsed ELDOR data. *Appl. Magn. Reson. 30*, 473−498.
(29) Stoll, S., and Schweiger, A. (2006) EasySpin, a comprehensive software package for spectral simulation and analysis in EPR. *J. Magn. Reson. 178*, 42−55.
(30) Jeschke, G. (2002) Distance measurements in the nanometer range by pulse EPR. *ChemPhysChem 3*, 927−932.
(31) Jeschke, G., Bender, A., Paulsen, H., Zimmermann, H., and Godt, A. (2004) Sensitivity enhancement in pulse EPR distance measurements. *J. Magn. Reson. 169*, 1−12.
(32) Jeschke, G., Koch, A., Jonas, U., and Godt, A. (2002) Direct conversion of EPR dipolar time evolution data to distance distributions. *J. Magn. Reson. 155*, 72−82.
(33) Le Breton, N., Martinho, M., Mileo, E., Etienne, E., Gerbaud, G., Guigliarelli, B., and Belle, V. (2015) Exploring intrinsically disordered proteins using site-directed spin labeling electron paramagnetic resonance spectroscopy. *Frontiers in molecular biosciences 2*, 21.
(34) Biertumpfel, C., Yang, W., and Suck, D. (2007) Crystal structure of T4 endonuclease VII resolving a Holliday junction. *Nature 449*, 616−U614.
(35) Gorecka, K. M., Komorowska, W., and Nowotny, M. (2013) Crystal structure of RuvC resolvase in complex with Holliday junction substrate. *Nucleic Acids Res. 41*, 9945−9955.
(36) Liu, Y. J., Freeman, A. D. J., Declais, A. C., Wilson, T. J., Gartner, A., and Lilley, D. M. J. (2015) Crystal Structure of a Eukaryotic GEN1 Resolving Enzyme Bound to DNA. *Cell Rep. 13*, 2565−2575.

DOI: 10.1021/acs.biochem.6b00242
Biochemistry 2016, 55, 4166−4172